Research Article – JTEN – 2015 – 36

Journal of Thermal Engineering
Yildiz Technical University Press, Istanbul, Turkey
Vol. 2, No. 2, pp. 683-692, April, 2016.

http://eds.yildiz.edu.tr/journal-of-thermal-engineering/Articles
Manuscript Received April 21, 2015; Accepted June 03, 2015

This paper was recommended for publication in revised form by Regional Editor Balaram Kundu

COMPUTATION OF OPTIMUM PARAMETERS OF A HALF EFFECT WATER-LITHIUM BROMIDE VAPOUR ABSORPTION REFRIGERATION SYSTEM

Akhilesh Arora
Department of Mechanical Engineering, Delhi Technological University
Delhi, Delhi, India

***Manoj Dixit**
Centre for Energy Studies,
Indian Institute of Technology Delhi
New Delhi, Delhi, India

S.C. Kaushik
Centre for Energy Studies,
Indian Institute of Technology Delhi
New Delhi, Delhi, India

Keywords: Half effect, exergy analysis, Vapour Absorption Refrigeration, Water-lithium bromide
* *Corresponding author:* Phone: 91-9540660289
E-mail address: mandix@ces.iitd.ac.in

ABSTRACT

In this research paper, energy and exergy analyses of water lithium bromide half effect vapour absorption refrigeration system has been carried out. Based on energy and exergy analysis the optimum intermediate pressure is computed corresponding to maximum values of coefficient of performance and exergetic efficiency under various operating conditions. It is found that the optimum intermediate pressure corresponding to maximum values of coefficient of performance and exergetic efficiency is same. The effects of low and high pressure generator temperatures, evaporator temperature, effectiveness of solution heat exchangers and difference between low and high pressure generator temperatures have been considered in computing optimum intermediate pressure. The maximum COP varies between 0.415 - 0.438 and maximum exergetic efficiency varies between 6.96-13.74%.

INTRODUCTION

Refrigeration and air-conditioning systems have a major impact on energy demand with nearly 30% of the total energy consumption in the world (Buzelin et al., 2005). The fast depletion of fossil fuels has led the scientists to search for refrigeration systems that consume less high grade energy for their operation. The vapour absorption refrigeration (VAR) systems are a good option in this context. Arivazhagan, Saravanan and Renganarayanan (2006) expressed that low temperature heat sources such as waste heat, low pressure steam, solar heat, geothermal energy, etc. can be used as input in the absorption machines. A half effect absorption cooling cycle promises the utilization of low temperature heat source such as geothermal energy or waste heat available at 60ºC to 80ºC (Herold, Radermacher and Klein, 1996). Many researches have reported theoretical and experimental works on single and double effect absorption systems in the recent years. However the literature on half effect VAR systems is scant. Ma and Deng (1996) carried out theoretical analysis of low-temperature hot source driven two-stage half effect water lithium bromide absorption refrigeration system. The effects of varying hot water and chilled water temperatures on COP of the system have been examined. Their results revealed that the COP of half effect cycle is lower than that of single effect VAR system using water lithium bromide. Sumathy, Huang and Li (2002) developed a model of two-stage lithium bromide solar absorption chiller and reported that two stage chiller could be driven by low temperature hot water ranging from 60 to 75°C. Arivazhagan et al. (2005) carried out simulation studies of a half effect vapour absorption cycle using R134a-DMAC refrigerant-absorbent pair with low temperature heat sources for cold storage applications. The intermediate pressure of the cycle was optimized for maximum COP. It was reported that the effect of the temperature of the low absorber on the performance is more pronounced than that of the high absorber. The COP for the baseline system was found to vary from 0.35 for low evaporating and high condensing temperatures to 0.46 for high evaporating and low condensing temperatures. The second law efficiency was reported to be varying between 28-

44% for the sink temperature less than 30°C. Arivazhagan, Saravanan and Renganarayanan (2006) carried out experimental investigations of a half effect vapour absorption cycle using R134a-DMAC refrigerant-absorbent pair. The performance of the system in terms of degassing range, coefficient of performance and second law efficiency was examined. The system was able to operate at as low as -7°C evaporator temperature with generator temperatures varying from 55 to 75°C. The degassing range kept in high absorber was 40% more than in low absorber when the high absorber is operated at optimum intermediate pressure.

Domínguez-Inzunza et al. (2014) studied the performance of single-effect, half-effect and double-effect in series, double-effect inverse and triple-effect absorption cooling systems operating with ammonia-lithium nitrate. The COP obtained was 0.3 for half effect systems at the lowest evaporator and generator temperatures Crepinsek, Goricanec and Krope (2009) examined the performance on the basis of coefficient of performance and circulation ratio of single effect and half effect absorption refrigeration cycles for refrigeration temperatures below 0°C. The focus, in this paper, was to compare performances of the ammonia-water and possible alternative refrigerant absorbent pairs viz. ammonia-lithium nitrate, ammonia sodium thiocyanate, monomethylamine-water, R22-DMEU, R32-DMEU, R124-DMEU, R152a-DMEU, R125-DMEU, R134a-DMEU, trifluoroethanol (TFE)-tetraethylenglycol dimethyl ether (TEGDME), methanol-TEGDME and R134a-DMAC.

Gebreslassie, Medrano and Boer (2010) carried out exergy analysis for single, double, triple and half effect Water–Lithium bromide absorption cycles and calculated unavoidable exergy destruction. Their study did not include the computation of optimal values of intermediate pressure in half effect cycle. Gomri (2010) used solar energy as a heat source for computing the performance of a 10 kW capacity two stage half-effect absorption cooling system. The performance was computed based on the energy and exergy analysis principles.

Thus it is obvious from the literature review that the studies carried out on half effect VAR system are either theoretical (based on energy analysis) using water lithium bromide as refrigerant absorbent pair or experimental wherein the R134a-DMAC and many other absorbent refrigerant pairs are used.

In the works mentioned above, none of the researchers explained logically about the variation of various parameters. The criteria of the researchers for the analysis was to compute either the COP or the exergetic efficiency of the half effect LiBr- H_2O vapour absorption refrigeration system. None of the researcher examined the optimum performance parameters for the operation of the system for water lithium bromide system. The optimum parameters include the intermediate system pressure (i.e. LP generator pressure or HP absorber pressure), maximum COP, maximum exergetic efficiency, optimum solution circulation ratio in LP and HP circuits and effect of heat exchanger effectiveness on the maximum COP and maximum exergetic efficiency.

Considering the above facts, the objective of the present work is chosen to be the energy and exergy analysis of the water lithium bromide half effect VAR system. The energy and exergy analyses are carried out to compute the optimum intermediate pressure corresponding to maximum COP and maximum exergetic efficiency. The effects of LP and HP generators temperatures, absorber temperature, evaporator temperature and effectiveness of solution heat exchangers are studied on optimum solution circulation ratio, maximum COP and maximum exergetic efficiency of the system.

DESCRIPTION OF HALF EFFECT VAR SYSTEM

The half effect water lithium bromide absorption refrigeration system shown schematically in Fig. 1 comprises of an evaporator, LP & HP absorbers, LP & HP generators, LP and HP solution heat exchangers, condenser, solution pumps and solution and refrigerant throttle valves. The condenser and HP generator operate at same pressure which is the highest system pressure. The HP absorber and LP generator operate at same intermediate pressure whereas the LP absorber and evaporator operate at same lowest system pressure. Following relationship exists among the pressures in these components:

$$(P_{g\_h} = P_c) > (P_{g\_l} = P_{a\_h}) > (P_{a\_l} = P_e)$$

The refrigerant (water) is circulated through the evaporator, LP absorber, LP generator, HP absorber, HP generator and condenser. After water vapour has condensed in the condenser, it returns to the evaporator through an expansion valve. However, the absorbent lithium bromide aqueous solution is circulated within two separate stages i.e. a LP stage between the LP absorber and the LP generator, and a HP stage between the HP absorber and the HP generator. Compared to a single-stage absorption refrigeration system, there are two additional components viz. HP absorber and LP generator in a half effect system. These are used to concentrate the lithium bromide aqueous solution in the LP stage cycle.

THERMODYNAMIC ANALYSIS

Following assumptions are made for the analysis : Heat losses through the system components are negligible; and reference enthalpy (h_o) and entropy (s_o) used for calculating exergy of the working fluid are the values for water at an environmental temperature and pressure of 25°C and 1 bar respectively. For the computing the optimum parameters of half effect VAR system, the principles of mass and material conservation, energy balance (First law of thermodynamics) and exergy balance

(Second law of thermodynamics) are applied to each component of the system. Each component has been treated as a control volume with inlet and outlet streams, heat transfer and work interactions. The application of above mentioned principles is presented in the following equations.

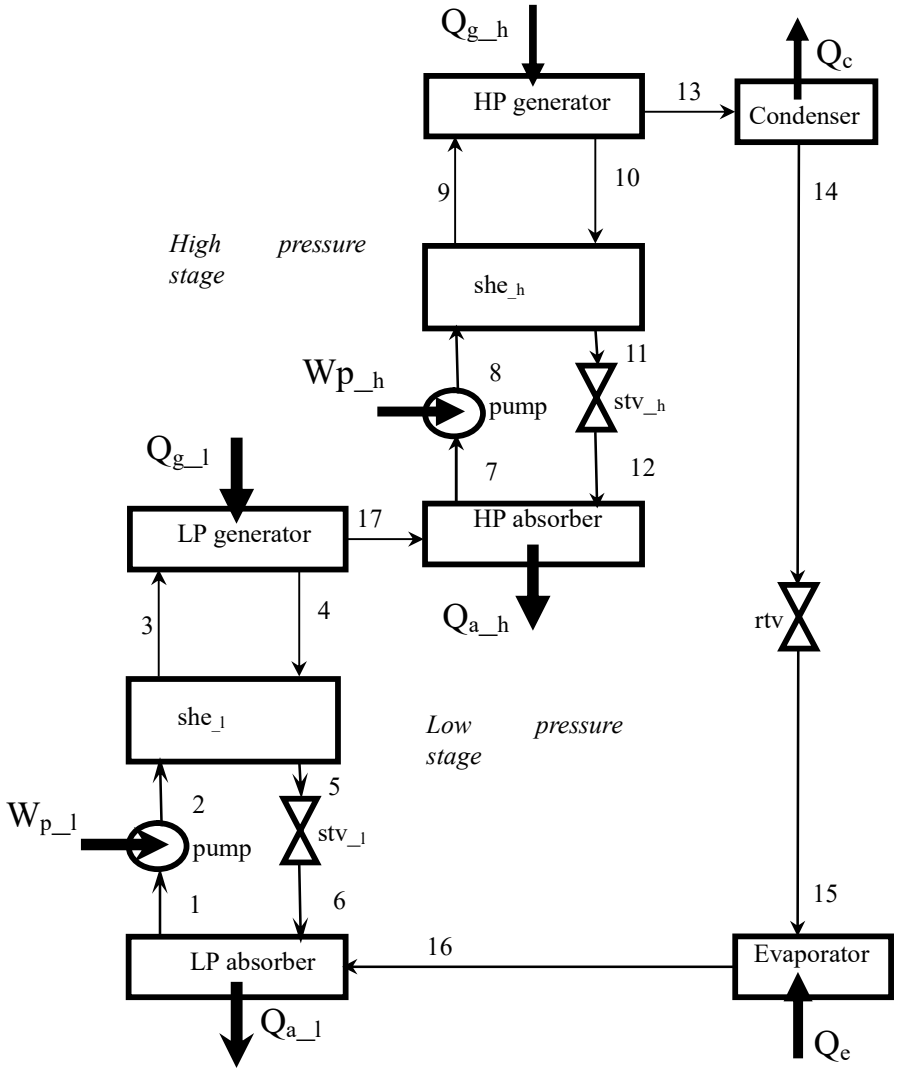

Fig. 1 Schematic diagram of a half effect water lithium bromide VAR system

Mass balance

The governing equations of mass and material conservation for a steady state and steady flow system are given below:

$$\sum \dot{m}_i = \sum \dot{m}_e \tag{1}$$

The equations of mass balance in a Half Effect system are specified below.

LP generator or LP absorber

$$\dot{m}_{g,l} = \dot{m}_{w,l} + \dot{m}_r \tag{2}$$

HP generator or HP absorber

$$\dot{m}_{g,h} = \dot{m}_{w,h} + \dot{m}_r \tag{3}$$

The mass flow rate of refrigerant through evaporator is $\dot{m}_r$.

Material Balance

LP generator or LP absorber

$$\dot{m}_{s,l} X_{s,l} = \dot{m}_{w,l} X_{w,l} \quad (4)$$

HP generator or HP absorber

$$\dot{m}_{s,h} X_{s,h} = \dot{m}_{w,h} X_{w,h} \quad (5)$$

Energy Balance

The first law of thermodynamics yields the energy balance of each component of the VAR system as follows:

$$\sum(\dot{m}_e h_e) - \sum(\dot{m}_i h_i) + \sum \dot{Q}_i = \dot{W} \quad (6)$$

The energy in each component of a Half Effect system is given by the following equations:

$$\dot{Q}_{a,l} = \dot{m}_r h_{16} + \dot{m}_{w,l} h_6 - \dot{m}_{s,l} h_1 \quad (7)$$

$$\dot{Q}_{g,l} = \dot{m}_r h_{17} + \dot{m}_{w,l} h_4 - \dot{m}_{s,l} h_3 \quad (8)$$

$$\dot{Q}_{a,h} = \dot{m}_r h_{17} + \dot{m}_{w,h} h_{12} - \dot{m}_{s,h} h_7 \quad (9)$$

$$\dot{Q}_{g,h} = \dot{m}_r h_{13} + \dot{m}_{w,h} h_{10} - \dot{m}_{s,h} h_9 \quad (10)$$

$$\dot{Q}_c = \dot{m}_r (h_{13} - h_{14}) \quad (11)$$

$$\dot{Q}_e = \dot{m}_r (h_{16} - h_{15}) \quad (12)$$

$$\dot{Q}_{shx,l} = \dot{m}_{s,l} (h_3 - h_2) = \dot{m}_{w,l} (h_4 - h_5) \quad (13)$$

$$\dot{Q}_{shx,h} = \dot{m}_{s,h} (h_9 - h_8) = \dot{m}_{w,h} (h_{10} - h_{11}) \quad (14)$$

$$\dot{W}_{p,l} = \dot{m}_{s,l} (h_2 - h_1) \quad (15)$$

$$\dot{W}_{p,h} = \dot{m}_{s,h} (h_8 - h_7) \quad (16)$$

$$Energy\ input = \dot{Q}_{g,l} + \dot{Q}_{g,h} + \dot{Q}_e + \dot{W}_{p,l} + \dot{W}_{p,h} \quad (17)$$

$$Energy\ output = \dot{Q}_{a,l} + \dot{Q}_{a,h} + \dot{Q}_c \quad (18)$$

The coefficient of performance (COP) of the Half Effect VAR system is defined as the ratio of the cooling capacity obtained at the evaporator divided by energy input into the high and low pressure generators and pumps. Accordingly, COP is given by Eq. (19).

$$COP = \frac{\dot{Q}_e}{\dot{Q}_{g,l} + \dot{Q}_{g,h} + \dot{W}_{p,l} + \dot{W}_{p,h}} \quad (19)$$

The solution circulation ratio (SCR) is defined as the ratio of the mass flow rate of the strong solution to the mass flow rate of the refrigerant. The solution circulation ratio of the low pressure and high pressure stages are given by the equations (20) and (21) respectively.

$$SCR_l = \frac{\dot{m}_{s,l}}{\dot{m}_r} = \frac{x_{w,l}}{x_{w,l} - x_{s,l}} \quad (20)$$

$$SCR_h = \frac{\dot{m}_{s,h}}{\dot{m}_r} = \frac{x_{w,h}}{x_{w,h} - x_{s,h}} \quad (21)$$

Exergy Balance

Exergy destruction in each component of a Half Effect Generation VAR system is furnished below:

$$\dot{E}D_{a\_l} = \dot{m}_r (h_{16} - T_o s_{16}) + \dot{m}_{w\_l} (h_6 - T_o s_6) - \dot{m}_{s\_l} (h_1 - T_o s_1) \quad (22)$$

$$\dot{E}D_{g\_l} = \dot{m}_{s\_l} (h_3 - T_o s_3) - \dot{m}_{w\_l} (h_4 - T_o s_4) - \dot{m}_r (h_{17} - T_o s_{17}) + \dot{Q}_{g\_l} (1 - T_0 / T_{g\_l}) \quad (23)$$

$$\dot{E}D_{a\_h} = \dot{m}_r (h_{17} - T_o s_{17}) + \dot{m}_{w\_h} (h_{12} - T_o s_{12}) - \dot{m}_{s\_h} (h_7 - T_o s_7) \quad (24)$$

$$\dot{E}D_{g\_h} = \dot{m}_{s\_h} (h_9 - T_o s_9) - \dot{m}_{w\_h} (h_{10} - T_o s_{10}) - \dot{m}_r (h_{13} - T_o s_{13}) + \dot{Q}_{g\_h} (1 - T_0 / T_{g\_h}) \quad (25)$$

$$\dot{E}D_c = \dot{m}_r ((h_7 - h_8) - T_o (s_7 - s_8)) \quad (26)$$

$$\dot{E}D_e = \dot{m}_r ((h_9 - h_{10}) - T_o (s_9 - s_{10})) + Q_e \left(1 - \frac{T_o}{T_r}\right) \quad (27)$$

$$\dot{E}D_{she\_l} = \dot{m}_{s\_l}((h_2 - h_3) - T_o(s_2 - s_3)) + \dot{m}_{w\_l}((h_4 - h_5) - T_o(s_4 - s_5)) \quad (28)$$

$$\dot{E}D_{she\_h} = \dot{m}_{s\_h}((h_8 - h_9) - T_o(s_8 - s_9) + \dot{m}_{w\_h}((h_{10} - h_{11}) - T_o(s_{10} - s_{11})) \quad (29)$$

$$\dot{E}D_{rtv} = \dot{m}_r T_o(s_{15} - s_{16}) \quad (30)$$

$$\dot{E}D_{stv\_l} = \dot{m}_{w\_l} T_o(s_6 - s_5) \quad (31)$$

$$\dot{E}D_{stv\_h} = \dot{m}_{w\_h} T_o(s_{12} - s_{11}) \quad (32)$$

$$\dot{E}D_t = \dot{E}D_{a\_l} + \dot{E}D_{a\_h} + \dot{E}D_{g\_l} + \dot{E}D_{g\_h} + \dot{E}D_c + \dot{E}D_e + \dot{E}D_{she\_l} + \dot{E}D_{she\_h} + \dot{E}D_{rtv} + \dot{E}D_{stv\_l} + \dot{E}D_{stv\_h} \quad (33)$$

Exergetic Efficiency

$$\eta_{e_x} = \frac{\dot{Q}_e\left|(1 - T_0/T_r)\right|}{\dot{Q}_{g\_l}\left(1 - T_0/T_{g\_l}\right) + \dot{W}_{p\_l} + \dot{Q}_{g\_h}\left(1 - T_0/T_{g\_h}\right) + \dot{W}_{p\_h}} \quad (34)$$

The base parameters considered for computation of results are evaporator temperature (T_e) = 7°C, condenser temperature (T_c) = 37.8°C, absorber temperature in low and high pressure stages ($T_{a\_l} = T_{a\_h}$) = 37.8°C, effectiveness of solution heat exchangers = 0.7, mass flow rate of refrigerant (water) = 1 kg/s.

RESULTS AND DISCUSSION

The results of the present analysis have been compared with the results of Ma and Deng (1996). It is observed that the COP in the present work is about 5% higher than the value obtained in their work. The difference in values is due to the fact that the properties of water lithium bromide have been taken from McNeely (1985) whereas in the present study the water lithium bromide properties are referred from Pa´tek and Klomfar (2006). Moreover, the values of heat exchanger effectiveness have not been reported by them whereas in the present work the same have been considered as 0.7.

Figure 2 presents the effect of variation in LP and HP generator temperatures on COP and exergetic efficiency of the Half Effect Generation VAR system. A small increase in the generator temperatures above 60.5°C causes the COP and exergetic efficiency values to increase abruptly. With further increase in HP and LP generator temperatures, the COP becomes constant whereas exergetic efficiency shows a decreasing trend. The initial values of COP and exergetic efficiency are nearly zero since the solution circulation ratio in HP stage is very high and consequently heat duty rate in HP generator is high. The maximum values of COP and exergetic efficiency obtained are about 0.41 and 9.5% respectively.

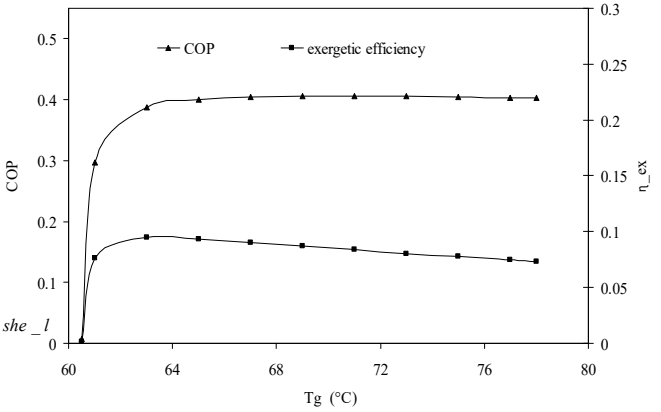

Fig. 2 Variation of COP and exergetic efficiency with generator temperature (T_e = 7°C, $T_{al} = T_{ah} = T_c$ = 37.8°C, $T_{gl} = T_{gh}$, $\varepsilon\_she_l = \varepsilon\_she_h$ =0.7)

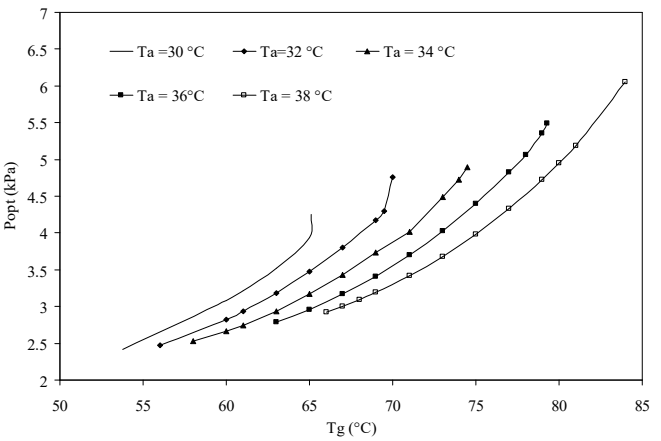

Fig. 3 Variation of optimum intermediate pressure (T_e = 7°C, $T_{a,l} = T_{a,h} = T_c$, $T_{g,l} = T_{g,h}$, $\varepsilon_{she,l} = \varepsilon_{she,h}$ =0.7)

Figure 3 illustrates the effect of generator temperature on optimum intermediate pressure for different absorber temperatures. For a constant absorber temperature, it is observed that with increase in generator temperature the optimum intermediate pressure increases. When generator temperature is increased beyond the value corresponding to maximum COP and maximum exergetic efficiency, then the requirement of heat in the generator increases resulting in fall of both COP and exergetic efficiency. Thus, in order to obtain the point of maximum COP and maximum exergetic efficiency corresponding to the increased generator temperature (at constant absorber temperature) the intermediate pressure has to be increased. Hence, optimum intermediate pressure increases

with increase in the generator temperature. For a constant value of generator temperature, the increase in absorber temperature is responsible for increase in solution circulation ratios and this causes the heat supply to increase in HP and LP generators. In order to maximize the COP and exergetic efficiency, the intermediate pressure should be reduced. So, optimum intermediate pressure decreases as absorber temperature increases.

Figure 4 presents the effect of generator temperature on maximum value of COP. It is observed that the maximum COP nearly remains constant with increase in generator temperature. This happens because the optimum pressure is adjusted in such a way that small reduction in heat supply in HP stage generator is observed whereas there is small increase in heat supply in LP generator. These two effects negate each other and hence maximum COP remains nearly constant.

As specified in previous paragraph that with increase in absorber temperature the optimum intermediate pressure is achieved for higher values of solution circulation ratios, hence more heat is to be supplied for the same generator temperature. Further, it is also observed that increase in condenser temperature causes more flashing during throttling in refrigerant throttle valve, hence cooling effect reduces marginally. Thus, increase in heat duty in generators and decrease in cooling effect in evaporator result in a decrease of COP when absorber and condenser temperatures increase. The maximum value of maximum COP achieved is about 0.438 (corresponding to $T_{a,h} = T_{a,l} = T_c = 30^oC$) whereas minimum value of maximum COP achieved is about 0.415(corresponding to $T_{a\_h} = T_{a\_l} = T_c = 38^oC$)

The variation of maximum exergetic efficiency is shown in Fig. 5. It is observed that with increase in HP and LP generator temperatures, maximum exergetic efficiency reduces. This happens because of increase in total irreversibility. The irreversibility in generators increase, since the temperature difference between the solution exiting the solution heat exchanger and generator increases. The irreversibility in absorbers also increase because of the weak solution which leaves the solution heat exchangers is at a temperature higher than before and hence the temperature difference between refrigerant and weak solution increases causing an increase in entropy generation and consequently higher exergy destruction is observed in absorbers. The irreversibility in condenser also increases because of increase in average temperature of condenser. The change in exergy destruction in valves is negligible. Thus increase in total exergy destruction is observed for the same output exergy and hence maximum exergetic efficiency decreases. The increase in absorber temperature causes increase in solution circulation ratio in LP and HP stages and consequently exergy destruction increase causing the maximum exergetic efficiency to reduce. The maximum and minimum values of maximum exergetic efficiency obtained are 13.74% and 6.96% under identical set of conditions as specified in previous paragraph.

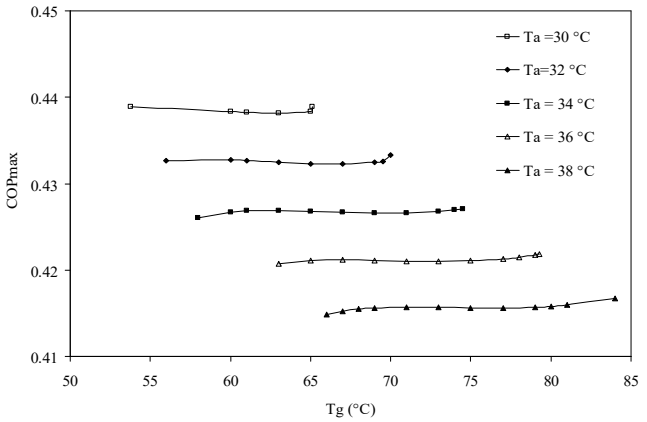

Fig. 4 Variation of maximum COP with generator temperature (T_e = 7°C , $T_{a,l} = T_{a,h} = T_c$, $T_{g,l} = T_{g,h}$, $\varepsilon_{she,l} = \varepsilon_{she,h} = 0.7$, $P_{g,l} = P_{a,h} = P_{opt}$)

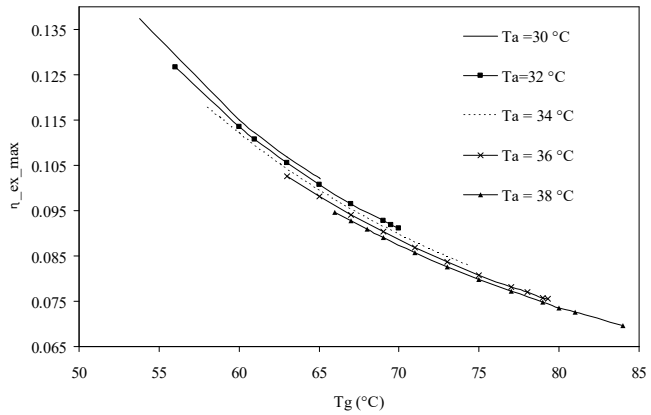

Fig. 5 Variation of maximum exergetic efficiency with generator temperature (T_e = 7°C, $T_{a,l} = T_{a,h} = T_c$, $T_{g,l} = T_{g,h}$, $\varepsilon_{she,l} = \varepsilon_{she,h} = 0.7$)

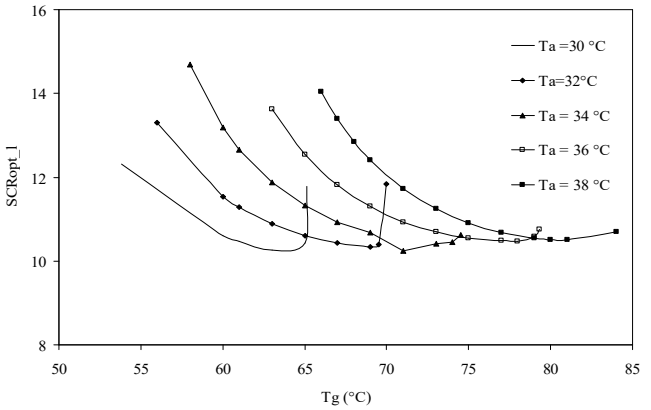

Fig. 6 Variation of optimum solution circulation ratio in LP stage with generator temperature (T_e = 7 °C, $T_{a,l} = T_{a,h} = T_c$, $T_{g,l} = T_{g,h}$, $\varepsilon_{she,l} = \varepsilon_{she,h}$ =0.7)

Figures 6 and 7 illustrate the variation in optimum solution circulation ratio in LP and HP stages with generator temperature. It is observed that the optimum solution circulation ratio reduces with increase in generator temperature in HP stage up to a specific value of generator temperature and further increase in generator temperature causes the solution circulation ratio to drop suddenly. This can be explained on the basis that with increase in HP generator temperature the *'Xw_h'* keeps on increasing whereas *'Xs_l'* keeps on decreasing and correspondingly mass flow rates of weak as well as strong solution keeps on reducing in HP stage. Finally a limit reaches where the mass flow rate of weak solution is negligible and the mass of strong solution leaving the absorber is unity.

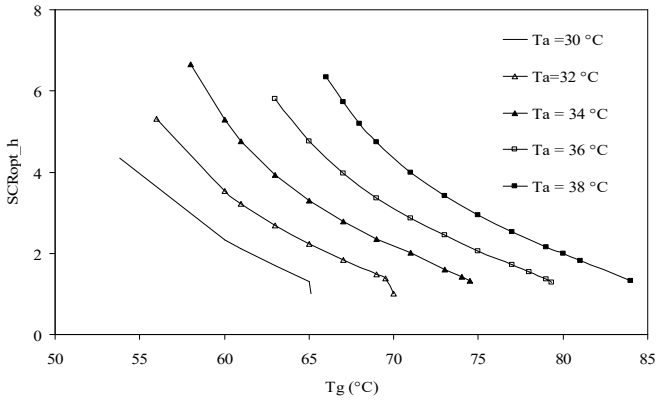

Fig. 7 Variation of optimum solution circulation ratio in HP stage with generator temperature *(*T_e = 7 °C, Tal = T_{ah} = T_c , T_{gl} = T_{gh}, ε_she_l =ε_she_h =0.7)

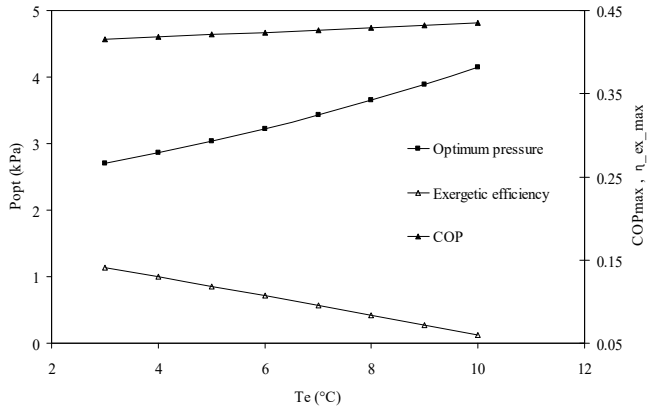

Fig. 8 Variation of optimum pressure, maximum COP and maximum exergetic efficiency with evaporator temperature (T_{ah} = T_{al} = T_c = 34°C, T_{gh} = T_{gl} = 67°C)

Thus the solution circulation ratio is nearly unity. Hence system can't be operated above this particular value of the solution circulation ratio since this is the minimum value which can be attained. Further it is also observed that the at this specific generator temperature, the optimum intermediate pressure (i.e. optimum pressure in HP absorber or LP generator) approaches condenser pressure. This is the reason for abrupt increase in the value of solution circulation ratio in LP stage.

Figure 8 illustrates the effect of evaporator temperature on optimum intermediate pressure, COP_{max} and maximum exergetic efficiency. It is observed that with increase in evaporator temperature, evaporator pressure increases and consequently optimum intermediate pressure also increases. The COP_{max} increases with increase in evaporator temperature because of reduction in solution circulation ratio in both LP and HP stages which causes heat supply rates to decrease in generators. The maximum exergetic efficiency reduces with increase in evaporator temperature. The results show a drop in both input and output exergies. However the rate of drop in output exergy per unit increase in evaporator temperature is found to be higher in comparison to rate of drop in input exergy per unit increase in evaporator temperature, hence exergetic efficiency, being a ratio of output exergy to input exergy, reduces.

Figure 9 shows the variation of optimum intermediate pressure in LP generator or HP absorber, COP_{max} and maximum exergetic efficiency versus effectiveness of solution heat exchangers. It is seen that the optimum intermediate pressure, COP_{max} and maximum exergetic efficiency increase with increase in effectiveness of solution heat exchangers. The COP_{max} and maximum exergetic efficiency increase because with increase in effectiveness of solution heat exchangers the heat supply at generators is reduced. Secondly, the irreversibility reduces as the temperature difference between the solution exiting the solution heat exchangers and generators reduce and it contributes in increasing the exergetic efficiency.

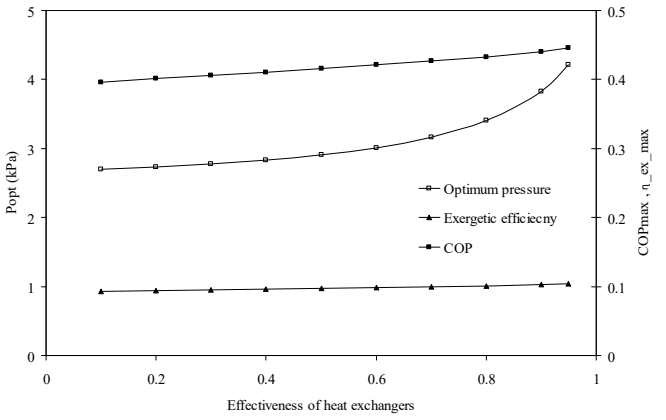

Fig. 9 Variation of optimum pressure, maximum COP and maximum exergetic efficiency with effectiveness of heat exchangers (T_{ah} = T_{al} = T_c = 34°C, T_{gh} = T_{gl} = 65°C, T_e = 7°C)

The variation of optimum intermediate pressure with variation in effectiveness of one of the solution heat exchanger (when the effectiveness of other heat exchanger is kept constant) is indicated in Fig. 10. The results indicate that when effectiveness of LP heat exchanger is assumed constant while effectiveness of HP heat exchanger is varied, the optimum intermediate pressure reduces and trends reverse when effectiveness of HP heat exchanger is assumed constant while effectiveness of LP heat exchanger is varied.

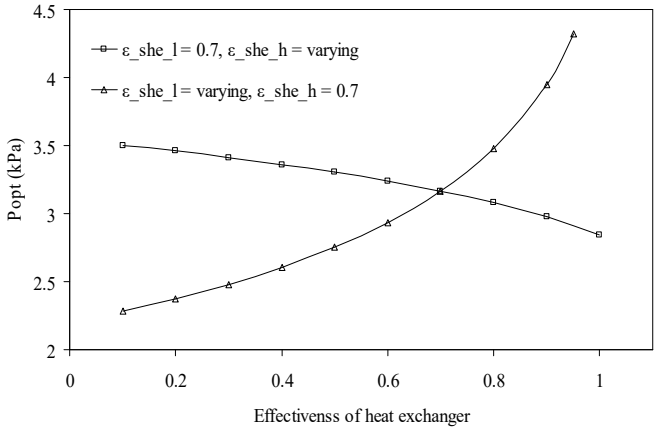

Fig. 10 Variation of optimum pressure with effectiveness of heat exchangers keeping the effectiveness of one heat exchanger constant ($T_{ah} = T_{al} = T_c = 34°C$, $T_{g,h} = T_{g,l} = 65°C$, $T_e = 7°C$)

Moreover, the effect of varying the effectiveness of LP heat exchanger is higher on both COP_{max} and maximum exergetic efficiency since the rate of rise of COP_{max} and maximum exergetic efficiency with increase in effectiveness of LP heat exchanger is higher in comparison to corresponding effect of increase in effectiveness of HP heat exchanger as shown in Fig. 11.

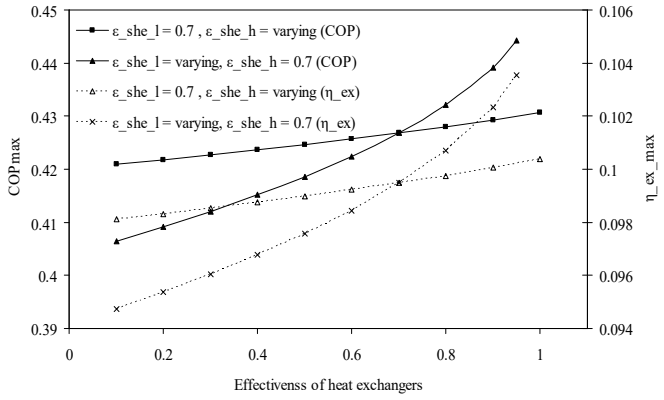

Fig. 11 Variation of maximum COP with effectiveness of heat exchangers ($T_{ah} = T_{al} = T_c = 34°C$, $T_{gh} = T_{gl} = 65°C$, $T_e = 7°C$)

Figure 12 shows the effect of HP generator temperature on COP and exergetic efficiency when it is taken higher and lower than the LP generator temperature. The results indicated in this Fig. show that it is better to have HP generator temperature lower than the LP generator temperature since maximum COP and maximum exergetic efficiency are higher when LP generator temperature is higher than HP generator temperature.

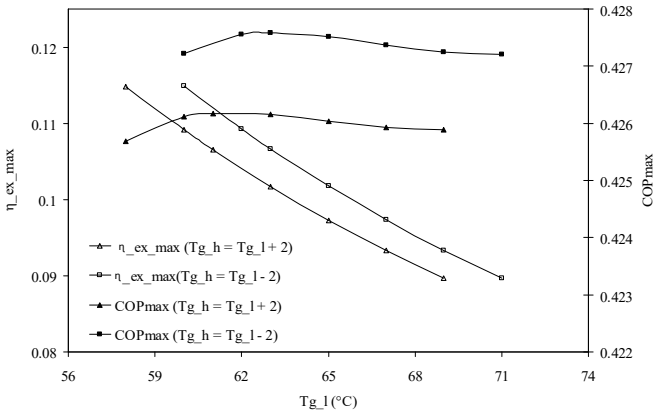

Fig. 12 Variation of maximum COP and maximum exergetic efficiency with generator temperature in LP stage ($T_{al} = T_{ah} = T_c = 34°C$, $T_e = 7°C$, $\varepsilon\_she_l = \varepsilon\_she_h = 0.7$, $P_{g,l} = P_{a,h} = P_{opt}$)

CONCLUSIONS

The main conclusions drawn on the basis of the analysis are listed below**:**

1. There exists a specific generator temperature below which a half effect system ceases to work. The COP and exergetic efficiency are zero corresponding to this value. In the present case, this value is found to be 60.5ºC corresponding to an intermediate pressure of 2 kPa (for Tc = Ta_l =Ta_h = 37.8C and Tg_h = Tg_l). The maximum value of COP achieved is about 0.41 and maximum exergetic efficiency attained is 9.5%. Such a trend of COP and exergetic efficiency is obtained only when the intermediate pressure (Pa_h or Pg_l) is not optimum.
2. There exists an optimum intermediate pressure (Pa_h_opt or Pg_l_opt) corresponding to which COP and exergetic efficiency are maximum. The optimum intermediate pressure increases with increase in LP or HP generator temperatures and evaporator temperature (at a particular absorber temperature) and decreases with increase in absorber temperature (at a particular generator temperature).
3. The variation in maximum COP (corresponding to optimum intermediate pressure) is negligible with increase in generator temperatures (for a particular absorber temperature) whereas maximum exergetic efficiency is found to decrease under identical set of conditions. The maximum COP and maximum exergetic efficiency reduce with increase in absorber temperature.
4. With the increase in evaporator temperature, the increase in maximum COP is negligible. The maximum exergetic efficiency reduces under identical conditions.
5. The increase in effectiveness of solution heat exchangers causes optimum intermediate pressure, maximum COP and

maximum exergetic efficiency to increase. Also, the influence of effectiveness of lower heat exchanger is more pronounced than that of higher heat exchanger.

6. The maximum COP and maximum exergetic efficiency are higher when LP generator temperature is higher in comparison to HP generator temperature.

NOMENCLATURE

COP	Coefficient of performance
e	Specific exergy (kJ/kg)
$\dot{E}$	Exergy rate of fluid (kW)
$\dot{E}D$	Exergy destruction rate (kW)
$\dot{E}F$	Exergy rate of fuel (kW)
$\dot{E}P$	Exergy rate of product (kW)
h	Enthalpy (kJ/kg)
HP	High pressure
LP	Low pressure
$\dot{m}$	Mass flow rate (kg/s)
P	Pressure (kPa)
$\dot{Q}$	Rate of heat transfer (kW)
s	Entropy (kJ/kg K)
SCR	Solution circulation ratio
T	Temperature (°C)
VAR	Vapour Absorption Refrigeration
$\dot{W}$	Work transfer rate (kW)
X	LiBr mass fraction
Subscripts	
a	Absorber
c	Condenser
e	Evaporator
ex	Exergetic
g	Generator
h	High temperature stage
l	Low temperature stage
max	Maximum
opt	Optimum
p	Pump
r	Refrigerant, room
rtv	Refrigerant throttle valve
s	Strong
she	Solution heat exchanger
t	Total
w	Weak
0	Dead state
Greek letters	
ε	Effectiveness
η	Efficiency
∑	Sum of

ACKNOWLEDGMENTS

The support of Ministry of New and Renewable Energy (MNRE), Government of India is duly acknowledged.

REFERENCES

[1] Vliet G.C., Lawson, M.B., Lithgow, R.A., 1982. Water-Lithium Bromide double effect absorption cooling system analysis. ASHRAE Transactions HO-82-5(2), 811-823.

[2] Fallek M., 1985. Parallel flow Chiller- heater. ASHRAE Transactions HI-85-41(5), 2095-2102.

[3] Kaushik S. C. and Chandra S., 1985. Computer modeling and parametric study of a double effect generation absorption refrigeration cycle. Energy Conversion Management 25(1), 9-14.

[4] Iyer, P. S. A, Murthy S. S. and Murthy M. V. K., 1988. Correlations for evaluation of the performance characteristics of vapour absorption refrigeration cycles. Solar & Wind Technology 5 (2), 191-197.

[5] Gommed K. and Grossman, G., 1990. Performance analysis of staged absorption heat pumps: water-lithium bromide systems. ASHRAE Transactions 30(6), 1590-1598.

[6] Riffat, S. B. and Shankland, N., 1993. Integration of absorption and vapour-compression systems. Applied Energy 46(4), 303-316.

[7] Oh M. D., Kim S. C., Kim Y. L. and Kim Y. I., 1994. Cycle analysis of an air-cooled LiBr/H_2O absorption heat pump of parallel-flow type. International Journal of Refrigeration 17(8), 556- 565.

[8] Xu G. P., Dai Y. Q., Tou K. W. and Tso C. P.,1996. Theoretical analysis and optimization of a double-effect series-flow-type absorption chiller. Applied Thermal Engineering 16(12), 975-987.

[9] Xu G. P. and Dai Y.Q., 1997. Theoretical analysis and optimization of a double-effect parallel flow type absorption chiller. Applied Thermal Engineering 17(2), 157-170.

[10] Arun M.B., Maiya M.P., Murthy S. S, 2000. Equilibrium low pressure generator temperatures for double effect series flow absorption refrigeration systems. Applied Thermal Engineering 20, 227-242.

[11] Elsafty A and Al-Daini A.J., 2000. Theoretical Investigation of a water-lithium bromide vapour absorption cooler, Renewables: The Energy for the 21st Century World Renewable Energy Congress VI, Brighton, UK, 2202-2205.

[12] Arun M.B., Maiya M.P., Murthy S. S, 2001. Performance comparison of double effect parallel flow and series flow water lithium bromide absorption systems. Applied Thermal Engineering 21, 1273-1279.

[13] Lee, S.F., Sherif, S.A., 1999. Second law analysis of multi effect Lithium Bromide/Water absorption chillers. ASHRAE Transactions Ch-99-23(3), 1256- 1266.

[14] Izquierdo M., Vega M. D, Lecuona A., Rodríguez P., 2000. Entropy generated and exergy destroyed in lithium bromide thermal compressors driven by the exhaust gases of an engine. International Journal of Energy Research 24(13), 1123 – 1140.

[15] Lee, S.F., Sherif, S.A., 2001. Second law analysis of various double effect Lithium Bromide/Water absorption chillers. ASHRAE Transactions AT-01-9(5), 664-673.
[16] Gebreslassie B.H., Medrano M., Boer D., 2010. Exergy analysis of multi-effect water LiBr/absorption systems: From half to triple effect. Renewable Energy 35, 1773–1782.
[17] Izquierdo M., Marcos J.D., Palacios M.E., González-Gil A., 2012. Experimental evaluation of a low-power direct air-cooled double-effect LiBr-H2O absorption prototype. Energy 37, 737-748.
[18] Farshi L.G., Mahmoudi S.M.S., Rosen M.A., Yari M., Amidpour M., 2013. Exergoeconomic analysis of double effect absorption refrigeration systems. Energy Conversion and Management 65, 13–25.
[19] Li Z., Ye X., Liu J., 2014. Performance analysis of solar air cooled double effect LiBr/H_2O absorption cooling system in subtropical city. Energy Conversion and Management 85, 302-312.
[20] Arcaklıoğlu E., Cavuşoğlu A. and Erişen A, 2005. An algorithmic approach towards finding better refrigerant substitutes of CFCs in terms of the second law of thermodynamics. Energy Conversion and Management 46, 1595-1611.
[21] Bejan, A., Tsatsaronis, G., Moran, M., 1996. Thermal Design and Optimization. John Wiley and Sons Inc., USA, 143–156.
[22] Klein S.A., Alvarado F., 2005. Engineering Equation Solver, Version 7.441, F-Chart software, Middleton, WI.
[23] Pátek J., Klomfar J., 2006. A computationally effective formulation of the thermodynamic properties of LiBr/H2O solutions from 273 to 500 K over full composition range. International Journal of Refrigeration 29, 566-578.